PHYSICAL REVIEW E **83**, 066401 (2011)

Electromagnetic field of a charge intersecting a cold plasma boundary in a waveguide

Tatiana Yu. Alekhina and Andrey V. Tyukhtin
Radiophysics Department of St. Petersburg University, 1 Ulyanovskaya, St. Petersburg 198504, Russia
(Received 27 January 2011; published 3 June 2011)

We analyze the electromagnetic field of a charge crossing a boundary between a vacuum and cold plasma in a waveguide. We obtain exact expressions for the field components and the spectral density of the transition radiation. With the steepest descent technique, we investigate the field components. We show that the electromagnetic field has a different structure in a vacuum than in cold plasma. We also develop an algorithm for the computation of the field based on a certain transformation of the integration path. The behavior of the field depending on distance and time and the spectral density depending on frequency are explored for different charge velocities. Some important physical effects are noted. A considerable increase and concentration of the field near the wave front in the plasma is observed for the case of ultrarelativistic particles. In the plasma, the mode envelopes and spectral density show zero points when the charge velocity is within certain limits.

DOI: 10.1103/PhysRevE.83.066401 PACS number(s): 41.60.Dk, 52.35.Hr

I. INTRODUCTION

The investigation of the transition radiation of a charge intersecting a boundary between different media has been ongoing since 1946 when it was predicted by V. L. Ginzburg [1]. Thereafter, many studies were published in this area (see, for example, [2]). Some aspects of this phenomenon, however, have not been analyzed sufficiently. This especially concerns the study of the structure of electromagnetic fields (in contrast to the energetic characteristics analyzed in detail for many problems [1–4]). Only over the last few years, the structure of the electromagnetic field has been considered for two unbounded media, in particular, in the case of the interface between a so-called left-handed medium and ordinary media [5–8]. Note that the analogous situation occurs in the investigation of Cherenkov radiation. Although it was discovered and explained in the 1930s [9], a sufficiently detailed description of the total field structure in a typical medium with resonant dispersion has been given only recently [8,10–12].

It should be noted that charge field structures in a regular waveguide with one or several media layers have been analyzed frequently (see, for example, [13–27]). The general theory for such problems was developed in [13], and many cases of different media (nondispersive dielectric [14–17], dielectric with resonant dispersion [18,19], dielectric with slight losses [20], active media [20–24], and metamaterials [25–27]) were considered. These investigations are related to the so-called wakefield accelerator technique [14–24]. In addition, some essential perspectives exist for developing new, nondestructive methods of charged particle beam diagnostics [25–27].

However, analogous problems in cases of irregular waveguides with two different media have rarely been analyzed, although they are important as well. The bunch inevitably intersects the boundary, and the fields that are generated during a certain time interval can be parasitic (for the wakefield acceleration technique), but useful (for new methods of particle detection and beam diagnostics; this was demonstrated for the interface between two unbounded media in [5–8]).

The number of problems considered in this area is very small. We can mention the investigation of the energetic characteristics of transition radiation in the cases of the boundary vacuum–cold-plasma [3,4] and vacuum–left-handed media [7] only. A description of the field structure is absent even in the case of a relatively simple medium, such as cold plasma. For this reason, it is important to analyze the electromagnetic field in a waveguide at the interface between a vacuum and a cold plasma. This is one of the key problems in electromagnetic radiation theory. It can be useful for the new methods of generation of superhigh frequency electromagnetic waves as well as for diagnostics of the charged particle beams. It should be emphasized also that, in such a situation, transition radiation is the only type of space radiation; consequently, it can be investigated *per se* (Cherenkov radiation is absent in the cold isotropic plasma). Our analysis is concentrated on finding the main peculiarities of the electromagnetic field structure. Therefore, we are restricted to a consideration of the simplest cylindrical waveguide. Note that a circular waveguide is also the basic structure for the majority of accelerators.

II. GENERAL RESULTS

Consider the electromagnetic field (EMF) generated by a point charged particle q moving in the waveguide of radius a along its axis through the interface ($z = 0$) between homogeneous isotropic dispersive media characterized by permittivity and permeability $\varepsilon_1(\omega)$ and $\mu_1(\omega)$, respectively, for $z < 0$, and $\varepsilon_2(\omega)$ and $\mu_2(\omega)$, respectively, for $z > 0$. The charge moves uniformly with a velocity $V = c\beta$ (c is the light velocity in a vacuum) and intersects the boundary at the moment $t = 0$ (Fig. 1).

The analytical solution of this problem is traditionally found for the spectral harmonics of the vector potentials $\vec{A}_{\omega 1,2} = A_{\omega 1,2}\vec{e}_z$ as an expansion into a series of eigenfunctions of the transversal operator. As an example, the transversal component of the electrical field is presented in the form:

$$E_{r1,2} = E^q_{r1,2} + E^b_{r1,2},$$

$$\begin{Bmatrix} E^q_{r1,2} \\ E^b_{r1,2} \end{Bmatrix} = \frac{2qa^{-3}}{\pi\beta c}\sum_{n=1}^{\infty}\frac{\chi_{0n}J_1(\chi_{0n}r/a)}{J_1^2(\chi_{0n})}\begin{Bmatrix} I^q_{1,2} \\ I^b_{1,2} \end{Bmatrix}, \quad (1)$$

$$I^q_{1,2} = \int_{-\infty}^{\infty}\frac{\exp[i\omega z/c\beta]}{\varepsilon_{1,2}\left(\omega^2/c^2\beta^2 - k^2_{z1,2}\right)}d\omega, \quad (2)$$

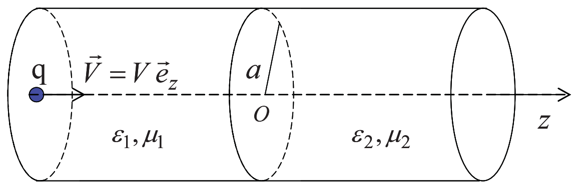

FIG. 1. (Color online) Geometry of the problem.

$$I^b_{1,2} = c\beta \int_{-\infty}^{\infty} \frac{B_{n1,2}k_{z1,2}\exp[-i(\omega t - k_{z1,2}|z|)]}{\omega\varepsilon_{1,2}g(\omega)} d\omega,$$

$$B_{n1,2} = \frac{\varepsilon_{1,2}}{\omega/c\beta \pm k_{z2,1}} - \frac{\omega\varepsilon_{2,1}/c\beta \mp \varepsilon_{1,2}k_{z2,1}}{\omega^2/c^2\beta^2 - k^2_{z1,2}}, \quad (3)$$

$$g(\omega) = \varepsilon_2 k_{z1} + \varepsilon_1 k_{z2}, \quad (4)$$

where $\omega_n = \chi_{0n}c/a$, χ_{0n} is the nth zero of the Bessel function $[J_0(\chi_{0n}) = 0]$, $k_{z1,2} = \sqrt{\omega^2 n^2_{1,2} - \omega_n^2}/c$ ($\mathrm{Im}k_{z1,2} > 0$), and $n^2_{1,2}(\omega) = \varepsilon_{1,2}(\omega)\mu_{1,2}(\omega)$.

The expressions found in (1) are decompositions in an infinite series of normal modes. Each of the modes includes a Fourier integral with respect to frequency. One can see that the electromagnetic field components have two summands. The first one ($E^q_{r1,2}$) is the field of the charge in the unbounded medium. V. L. Ginzburg [2] called it the "forced" field. It contains Cherenkov (or Vavilov-Cherenkov) radiation if the charge velocity exceeds the Cherenkov threshold. The second summand ($E^b_{r1,2}$) is the "free" field connected with the influence of the boundary. It includes transition radiation (TR).

If we rearrange the order of summation and integration in the expression for the forced field [(1), (2)], the series obtained can be summarized, as it was shown in [13]:

$$\frac{2}{a^2}\sum_{n=1}^{\infty} \frac{\chi_{0n}J_1(\chi_{0n}r/a)}{J_1^2(\chi_{0n})\left(\omega^2/\beta^2c^2 - k^2_{z1,2}\right)} = K_0(s_{1,2}r) - \frac{K_0(s_{1,2}a)}{I_0(s_{1,2}a)}I_0(s_{1,2}r), \quad (5)$$

where $s^2_{1,2} = \omega^2(\beta^2 n^2_{1,2} - 1)/\beta^2c^2$. Substituting (5) in Expression (1) for $E^q_{r1,2}$ gives the traditional expression for EMF of a charge in a waveguide with a homogeneous medium [13].

Further research associates the charge flying from a vacuum (medium 1) with $\varepsilon_1 = 1, \mu_1 = 1$ into cold plasma (medium 2). We assume that plasma is isotropic and the ion motion can be neglected. So, the following expressions are used for medium 2:

$$\varepsilon_2 = 1 - \omega_p^2(\omega^2 + 2i\omega\omega_d)^{-1}, \quad \mu_2 = 1, \quad (6)$$

where ω_p is a plasma frequency and ω_d is a small parameter responsible for absorption ($\omega_d \ll \omega_p$). If $\omega_d \to 0$, we have

$$k_{z1} = \sqrt{\omega^2 - \omega_n^2}/c, \quad k_{z2} = \sqrt{\omega^2 - \omega_n^2 - \omega_p^2}/c. \quad (7)$$

For the free field determined by $I^b_{1,2}$, we have the following expression:

$$I^b_{1,2} = \omega_p^2 c^2 \beta \int_{-\infty}^{\infty} f_{1,2}\exp[-i(\omega t - k_{z1,2}|z|)]d\omega, \quad (8)$$

where

$$f_1 = \frac{ck_{z1}[\omega(1-\beta^2) + c\beta k_{z2}]}{\tilde{g}(\omega)\left(\omega^2 - c^2\beta^2k^2_{z1}\right)(\omega + c\beta k_{z2})}, \quad (9)$$

$$f_2 = \frac{\omega c k_{z2}\left[\omega c\beta - \omega^2(1-\beta^2) - \beta^2\omega_p^2\right]}{\tilde{g}(\omega)(\omega^2 - \omega_p^2)} \times \left[\left(\omega^2 - c^2\beta^2k^2_{z2}\right)(\omega - c\beta k_{z1})\right]^{-1}, \quad (10)$$

$$\tilde{g}(\omega) = \left(\omega^2 - \omega_p^2\right)\sqrt{\omega^2 - \omega_n^2} + \omega^2\sqrt{\omega^2 - \omega_n^2 - \omega_p^2}. \quad (11)$$

Subsequent research regarding Expression (8) was carried out with analytical and computational methods. We are interested in the behavior of the field components depending on distance and time for different velocities of the motion of the charge.

III. ANALYTICAL INVESTIGATION FOR THE VACUUM AREA

In the analytical method, asymptotic expressions for the free field components of each mode can be obtained with the steepest descent technique, which was developed in detail in diffraction theory [28,29]. Such analysis is usually performed with the methods of the complex variable function theory. It has not been carried out before for the problem under consideration. We perform this analysis for the case of negligible losses taken into account for the determination of the location of the singularities of integrands only. The first step in such research is to study the singularities of integrands $f_{1,2}(\omega)$ in a complex plane. At first, we perform an analysis of the free field in the vacuum area $z < 0$. One can show that function $f_1(\omega)$ has the following singularities in a complex plane (ω):

(1) four branch points $\pm\tilde{\omega}^{(1)}_n = \pm\omega_n - i\delta_1$ and $\pm\tilde{\omega}^{(2)}_n = \pm\sqrt{\omega_n^2 + \omega_p^2} - i\delta_2$;

(2) four poles on the imaginary axis $\pm\omega^{(1)}_{0n} = \pm\frac{i\beta\omega_n}{\sqrt{1-\beta^2}}$ and $\pm\omega^{(2)}_{0n} = \pm\frac{i\beta\sqrt{\omega_n^2+\omega_p^2}}{\sqrt{1-\beta^2}}$;

(3) two poles at zero points of the function $\tilde{g}(\omega) \pm \Omega_n = \pm(\omega_n^2 + \omega_p^2/2 - \sqrt{\omega_n^2 + \omega_p^2}/2)^{1/2} - i\delta_3$.

Here, δ_1, δ_2, and δ_3 are positive infinitesimal quantities (it can be easily proven by taking into account weak absorption in a medium). Therefore, all of the singularities take place below a real axis [Fig. 2(a)]. Note that we have to define radicals (7) in accordance with the rules $\mathrm{Im}k_{z1,2} > 0$ on the real axis only. They can be defined arbitrarily in other parts of a complex plane. It is convenient for the next consideration to have the branch cuts as shown in Fig. 2. In the limit $\omega_d \to 0$, these cuts are defined with the equations:

$$\mathrm{Re}\sqrt{\omega^2 - \omega_n^2 - \omega_p^2} = 0, \quad \mathrm{Re}\sqrt{\omega^2 - \omega_n^2} = 0, \quad (12)$$

and the integration path goes along the upper edge of the branch cut. For obtaining asymptotic expressions, we use the steepest descent technique. Beforehand though, it is convenient to make the following replacement of variables:

$$\omega = \omega_n\cosh\chi, \quad \sqrt{\omega^2 - \omega_n^2} = \omega_n\sinh\chi. \quad (13)$$

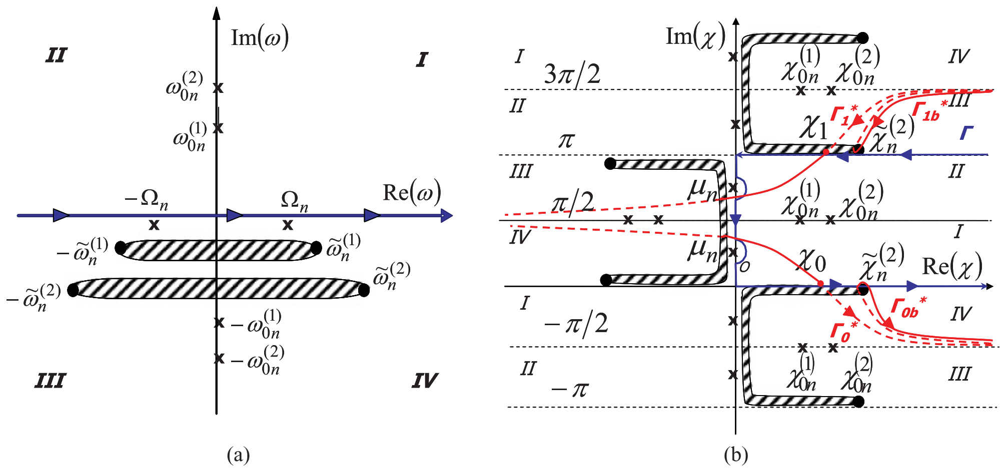

FIG. 2. (Color online) Disposition of singularities of integrands, branch cuts, and the integration path for I_1^b in a complex plane of (a) ω and (b) χ for the field in a vacuum (the case of $\mathrm{Re}\chi_{0,1} < \mathrm{Re}\tilde{\chi}_n^{(2)}$). The dashed parts of contour Γ^* are situated in the lower sheet of the Riemann surface.

(Note that this technique was used for the analysis of diffraction by a half plane in the flow of nondispersive medium [30]). This replacement removes the pair of branch points $\pm\tilde{\omega}_n^{(1)}$. The interaction between quadrants of the complex plane (ω) and areas in the plane (χ) is presented in Fig. 2 (with Roman numerals). The upper ("physical") sheet of the Riemann surface (ω) conforms to the right-half plane ($\mathrm{Re}\chi = \chi' > 0$) and the bottom sheet conforms to the left-half plane ($\chi' > 0$). The initial integration path in the plane (χ) is the contour Γ. The branch point $\tilde{\omega}_n^{(2)}$ and poles $\omega_{0n}^{(1)}$, $\omega_{0n}^{(2)}$, and Ω_n turn into $\tilde{\chi}_n^{(2)}$, $\chi_{0n}^{(1)}$, $\chi_{0n}^{(2)}$, and μ_n, respectively (Fig. 2).

There are two saddle points on contour Γ: χ_0 and $\chi_1 = \chi_0 + i\pi$, where $\cosh(\chi_0) = ct/R$, $R = \sqrt{c^2t^2 - z^2}$. The steepest descending paths (SDPs) consists of two branches (Γ_0^* and Γ_1^*) determined by the requirements:

$$\mathrm{Re}[F(\chi) - F(\chi_{0,1})] < 0, \quad \mathrm{Im}[F(\chi) - F(\chi_{0,1})] = 0, \quad (14)$$

where $F(\chi) = -i\omega_n R\cosh(\chi - \chi_0)/c$.

The poles and the branch points can be crossed in the transformation of contour Γ into a new contour Γ^* passing through the saddle points $\chi_{0,1}$, and the contributions from the corresponding singularities should be included in asymptotic expressions. So, if $\mathrm{Re}\chi_{0,1} > \mathrm{Re}\tilde{\chi}_n^{(2)}$, then there is no intersection of the branch points, and the contour Γ^* consists of two paths Γ_0^* and Γ_1^* only. However, in the case $\mathrm{Re}\chi_{0,1} < \mathrm{Re}\tilde{\chi}_n^{(2)}$, the saddle points lie on the edges of the branch cut, and in transformation of Γ into Γ^*, the branch points are crossed [Fig. 2(b)]. As a result, the new contour contains not only SDPs Γ_0^* and Γ_1^*, but also additional SDPs Γ_{0b}^* and Γ_{1b}^*, which consist of two branches situated in different Riemann surfaces. The estimation from the contributions of Γ_0^* and Γ_1^* is made by the saddle point approximation so far as the first derivatives of function $F(\chi)$ vanishes at the saddle points. As distinct from this, the contributions from Γ_{0b}^* and Γ_{1b}^* are evaluated by the Laplace method because these contours are SDPs running from the branch points where these derivatives are not 0. As a result, one can obtain the following approximate expression:

$$E_{r1} \approx \frac{2q\omega_p^2}{\pi c^2}\sum_{n=1}^{\infty}\frac{\chi_{0n}J_1(\chi_{0n}r/a)}{J_1^2(\chi_{0n})}(I_{10} + I_{1\Omega} + I_{1b}), \quad (15)$$

$$I_{10} \approx \sqrt{\frac{2\pi}{\Lambda}}\frac{\omega_n|z|}{R}2\mathrm{Re}\left\{f_1(\chi_0)\exp\left[-i\left(\frac{\omega_n R}{c} + \frac{\pi}{4}\right)\right]\right\}, \quad (16)$$

$$I_{1\Omega} \approx 2f_{1\Omega}\cos(\Omega_n t)\exp\left[-\frac{\sqrt{\omega_n^2 - \Omega_n^2}|z|}{c}\right] \times\Theta\left(\sqrt{\sqrt{1 - \omega_p^4/4\omega_n^4} - \omega_p^2/2\omega_n^2} - |z|/c\right), \quad (17)$$

$$I_{1b} \approx 2f_{1b}\cos\left(\sqrt{\omega_n^2 + \omega_p^2}t - |z|\,\omega_p/c\right) \times\left(\omega_p t - |z|\sqrt{\omega_n^2+\omega_p^2}/c\right)^{-3/2}\Theta\left(\omega_p ct - |z|\sqrt{\omega_n^2+\omega_p^2}\right), \quad (18)$$

where $\Theta(\xi)$ is the Heaviside function. This asymptotic expression is valid under the condition that $\Lambda = \omega_n R/c \gg 1$ and under the additional requirements that the saddle points are far enough from the poles and the branch points as follows: $|\Lambda - \Omega_n t - \sqrt{\omega_n^2 - \Omega_n^2}|z|/c| \gg 1$, $|\omega_p t - \sqrt{\omega_n^2+\omega_p^2}|z|/c| \gg \sqrt{\Lambda}$. If these requirements are not fulfilled, so-called "uniform asymptotic" expressions [28,29] can be obtained for the pole and branch cut contributions. The saddle point contributions I_{10} represent the space transition radiation that is determined by Formula (16). The pole contributions $I_{1\Omega}$ (17) exponentially decrease with the distance from the border at $z = 0$. Therefore, they can be called "surface standing waves." The branch cut contributions I_{1b} (18) also exist near the boundary and can be called "lateral standing waves" by analogy with the lateral waves known from diffraction theory [28]. It should be noted that the obtained asymptotic expressions are not valid if the saddle points are too close to the poles or to the branch points.

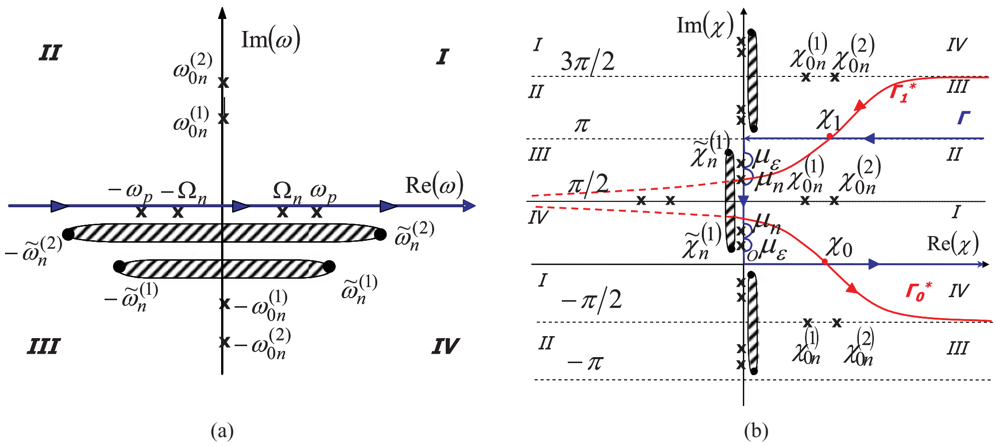

FIG. 3. (Color online) Disposition of the singularities of the integrands, corresponding branch cuts, and integration path in I_2^b in a complex plane of (a) ω and (b) χ for the free field in the plasma.

IV. ANALYTICAL INVESTIGATION FOR THE PLASMA AREA

A similar investigation can be made for the free field in cold plasma. As distinct from the vacuum, the integrand $f_2(\omega)$ (10) has an additional pair of poles: $\pm\omega_p - i0$ [apart from the singularities of the function $f_1(\omega)$]. The cuts are also drawn in the case of the vacuum. The location of the poles, branch points, corresponding branch cuts, and the initial integration path are presented in Fig. 3(a). It is convenient to make the following change of variables:

$$\omega = \sqrt{\omega_n^2 + \omega_p^2}\cosh\chi,$$
$$\sqrt{\omega^2 - \omega_n^2 - \omega_p^2} = \sqrt{\omega_n^2 + \omega_p^2}\sinh\chi. \qquad (19)$$

In Fig. 3(b), the initial integration path Γ, a SDP contour Γ^* (passing through the saddle points $\chi_{0,1}$), and the integrand singularities are shown [the branch points $\tilde{\omega}_n^{(2)}$ and poles $\omega_{0n}^{(1)}, \omega_{0n}^{(2)}$, Ω_n, and ω_p turn into $\tilde{\chi}_n^{(2)}$, $\chi_{0n}^{(1)}$, $\chi_{0n}^{(2)}$, μ_n, and μ_ε, respectively].

In the transformation of contour Γ into SDP Γ^*, as well as in the vacuum, the poles can be crossed. However, contrary to the vacuum, the branch points never intersect. One can obtain the following asymptotic expression for the free field in the plasma:

$$E_{r2} \approx \frac{2q\omega_p^2}{\pi c^2}\sum_{n=1}^{\infty}\frac{\chi_{0n}J_1(\chi_{0n}r/a)}{J_1^2(\chi_{0n})}(I_{20} + I_{2\Omega} + I_{2\varepsilon}), \qquad (20)$$

$$I_{20} \approx \sqrt{\frac{8\pi}{\Lambda_2}}\frac{\sqrt{\omega_n^2+\omega_p^2}|z|}{R}\cos\left(\frac{\sqrt{\omega_n^2+\omega_p^2}R}{c} + \frac{\pi}{4}\right), \qquad (21)$$

$$I_{2\Omega} \approx 2f_{2\Omega}\cos(\Omega_n t)\exp\left[-\sqrt{\omega_n^2+\omega_p^2-\Omega_n^2}|z|/c\right] \times \Theta\left(\sqrt{\sqrt{1-\omega_p^4/4(\omega_n^2+\omega_p^2)^2} - \omega_p^2/2(\omega_n^2+\omega_p^2)} - |z|/ct\right), \qquad (22)$$

$$I_{2\varepsilon} \approx 2f_{2\varepsilon}\cos(\omega_p t)\exp(-\omega_n|z|/c) \times \Theta\left(ct/R - \sqrt{1+\omega_n^2/\omega_p^2}\right). \qquad (23)$$

This asymptotic expression is valid under the condition that $\Lambda_2 = \sqrt{\omega_n^2+\omega_p^2}R/c \gg 1$ and under the additional requirements that $|\Lambda_2 - \omega_n t - \sqrt{\Omega_n^2+\omega_p^2-\omega_n^2}|z|/c| \gg 1$, $|\Lambda_2 - \omega_p t - \omega_n|z|/c| \gg 1$. This means that the saddle points and poles are sufficiently distant from one another. The saddle point contributions (21) give the space transition radiation. The pole contributions (22) and (23) allow the fields to decrease exponentially with the distance from the boundary. These are the "surface standing waves" and the "plasma oscillation," respectively. In summary, the structure of the electromagnetic field in the plasma differs from the structure in the vacuum: instead of contributions from two poles and two branch points (in vacuum), we have contributions from four poles (in the plasma).

V. METHOD OF COMPUTATION

For numerical calculations, the exact integral representations (8) are used. The efficient algorithm developed is based on a certain transformation of the initial integration path in the complex plane (ω). Earlier, such an algorithm was used for the computation of the field in different dispersive unbounded or semibounded media [6–8,12]. We demonstrate this method for the vacuum area. As shown at Fig. 4, the poles $\pm\Omega_n - i\delta_3$ are located near the integration path Γ. This leads to the rather abrupt behavior of the integrands in (8). The numerical algorithm is adapted for overcoming this difficulty. Note that Integral (8) can be written as an integral on a half-infinite contour Γ:

$$I_{1,2}^b = \int_{-\infty}^{\infty} f_{1,2}\exp[-i(\omega t - k_{z1,2}|z|)]d\omega$$
$$= 2\mathrm{Re}\left(\int_0^{\infty} f_{1,2}\exp[-i(\omega t - k_{z1,2}|z|)]d\omega\right). \qquad (24)$$

This formula follows directly from the reality of the field components, and it can be proven on the bases of the following properties: $(f_{1,2}(\omega))^* = f_{1,2}(-\omega^*)$, $(k_{z1,2}(\omega))^* = k_{z1,2}(-\omega^*)$. The symbol $*$ means a complex conjugation. Furthermore, we can transform this contour in an upper-half plane (ω) into

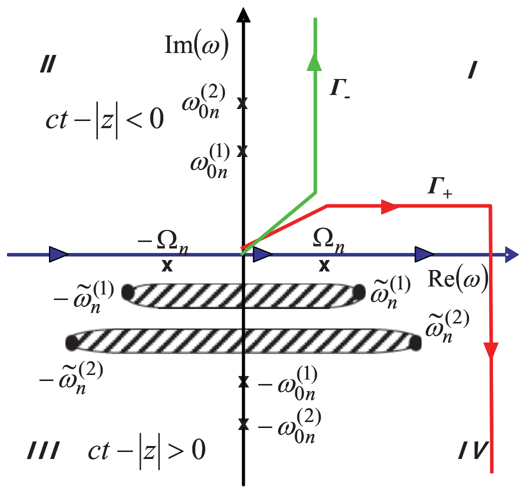

FIG. 4. (Color online) Disposition of the singularities of integrands $f_1(\omega)$, the corresponding branch cuts, and integration contours (initial and transformed) in a complex plane (ω) for the vacuum area.

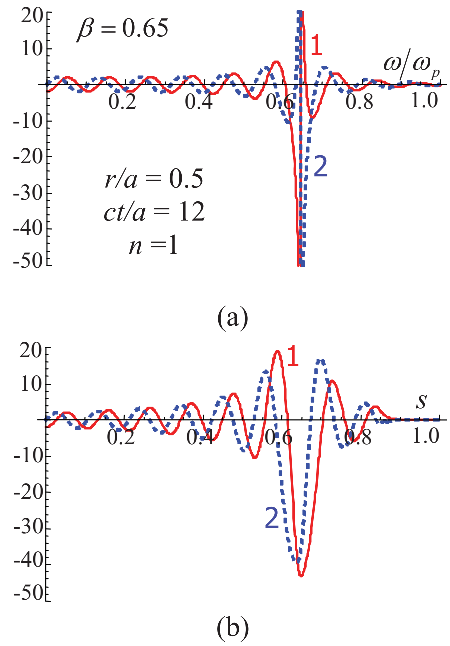

FIG. 5. (Color online) Behavior of the real (solid line 1) and imaginary (dashed line 2) parts of integrand of I_1^b for the vacuum area along the initial (top) and transformed (bottom) contours. s is a distance along path Γ_+. Curves along the initial contour have singularities. $ct/a = 12$, $r/a = 0.5$, $z/a = 0$, $n = 1$, $\beta = 0.65$.

contour Γ_- for $ct - |z| < 0$ (before the "wave front" $|z| = ct$) and in a lower-half plane into contour Γ_+ for $ct - |z| > 0$ (behind the wave front). These new contours should bypass all of the singularities (the poles and branch points) and then be matched with SDPs running parallel to an imaginary axis. The advantages of this integration in comparison with the initial contour (along the real axis) are that the behavior of the integrand is relatively smooth and decreases exponentially for large values of $|\omega|$ as it is shown at Fig. 5. Note that we can choose convenient parameters of contours for each computation.

VI. ENERGETIC SPECTRUM OF MODES

The important characteristics of the generated modes of the free field are their energetic spectrums. We consider the energy passing through the cross section of the waveguide in the first ($z < 0$) medium (Σ_1) and second medium (Σ_2) for all times during the charge's motion [3,4].

$$\Sigma_{1,2} = \int_{-\infty}^{\infty} dt \int_0^{2\pi} d\varphi \int_0^a r\,dr\, S_{z1,2},$$
$$S_{z1,2} = \frac{c}{4\pi} E_{r1,2} H_{\varphi 1,2}. \quad (25)$$

Expression (1) shows that every component of the electromagnetic field is an integral with respect to frequency and a sum of n modes. Thus, the values $\Sigma_{1,2}$ include a double sum of the products of n and m modes. However, the orthogonality of Bessel's functions results in zeroing all of the terms with $n \neq m$. Taking into account the fact that the integral with respect to φ gives 2π and the integral with respect to t gives a δ function $\delta(\omega + \omega')$, we have the following exact expression:

$$\Sigma_{1,2} = \int_0^{\infty} d\omega \sum_{n=1}^{\infty} w_{n1,2}, \quad (26)$$

where

$$w_{n1,2} = \frac{4q^2}{\pi a^4} \frac{\chi_{0n}^2 J_2^2(\chi_{0n})}{J_1^4(\chi_{0n})} \mathrm{Re}\Bigg\{ \left(\varepsilon_{1,2} c\beta \left|\chi_{0n}^2/a^2 - s_{1,2}^2\right|^2\right)^{-1}$$
$$\mp \frac{\exp[-i(\omega z/c\beta - k_{z1,2}|z|)]}{\varepsilon_{1,2}\omega\left(\chi_{0n}^2/a^2 - s_{1,2}^{2*}\right)} k_{z1,2} B_{n1,2}$$
$$+ \frac{\exp[i(\omega z/c\beta + k_{z1,2}^*|z|)]}{c\beta\varepsilon_{1,2}\left(\chi_{0n}^2/a^2 - s_{1,2}^2\right)} B_{n1,2}^*$$
$$\mp \frac{k_{z1,2}|B_{n1,2}|^2}{\varepsilon_{1,2}\omega} \exp[-\mathrm{Im}k_{z1,2}|z|]\Bigg\}. \quad (27)$$

So, the energies passing through the cross section of the waveguide are integrals with respect to ω, and the sum of the spectral energy densities of modes $w_{n1,2}$; $B_{n1,2}$ and $s_{1,2}$ are described with formulas (3) and (5), respectively. Integrals with half-infinite limits are obtained in (24). The first and last summands in (27) correspond to the forced and free fields. The second and the third summands are the interferential terms [3] that do not give essential contributions in $\Sigma_{1,2}$ for large values of z. Furthermore, the last addend (the spectral density of the transition radiation) is under investigation for the case of the boundary between the vacuum and the cold plasma (6). Following from (27) and (7), in the vacuum, the energy spectrum of the nth mode of TR is limited from below by ω_n, and, in the plasma, it exists at higher frequencies than $\sqrt{\omega_n^2 + \omega_p^2}$. One can show that w_{n2} has the zero point if the charge velocity is within the limits of $\beta_1 < \beta < \beta_2$,

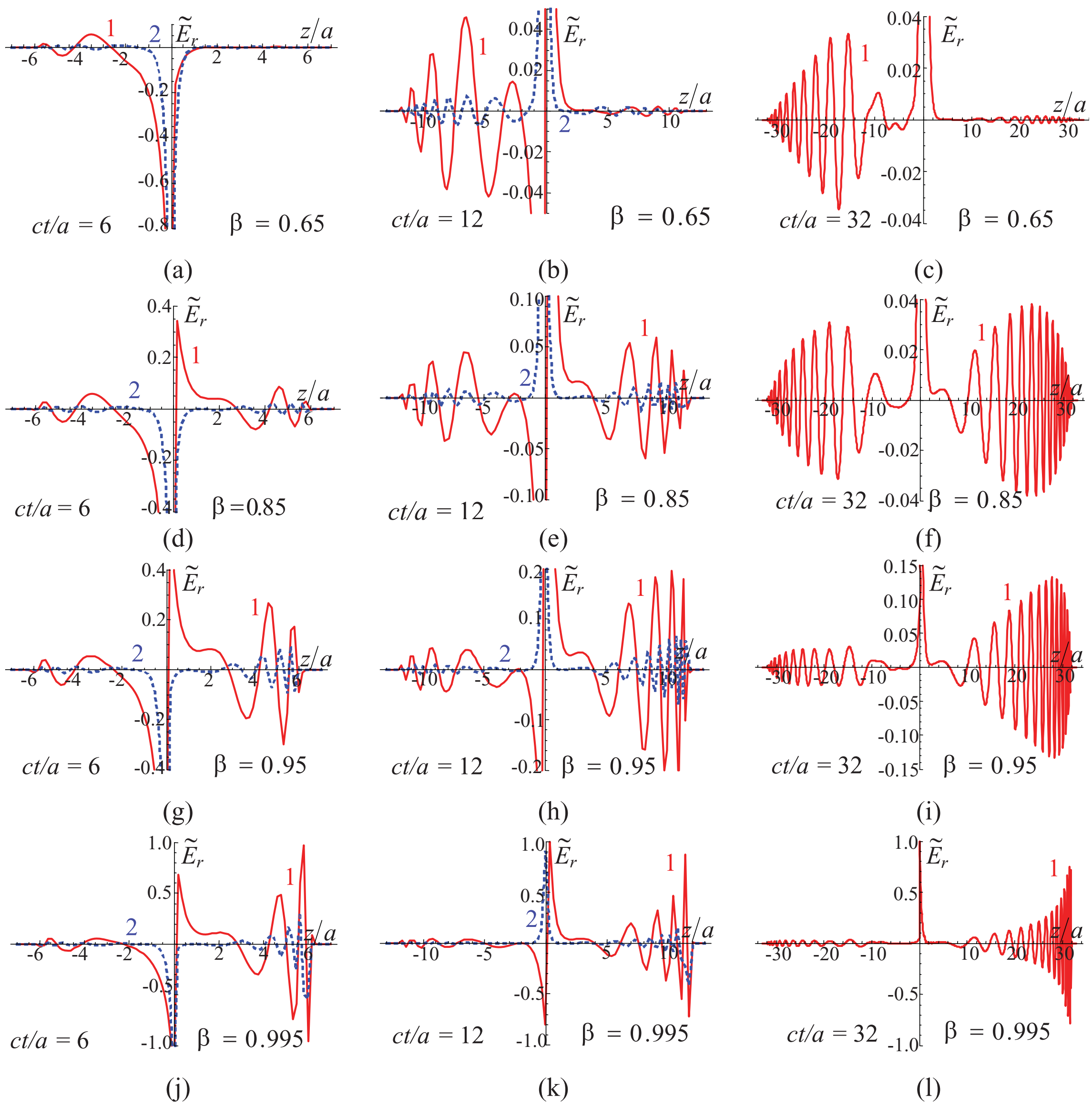

FIG. 6. (Color online) Dependence of normalized transversal component $\widetilde{E}_r = E_r \pi c^2/2q\omega_p^2$ of the first (continuous line 1) and second (dashed line 2) modes on distance z/a for different dimensionless times ct/a; $\beta = 0.65$ (the first row), $\beta = 0.85$ (the second row), $\beta = 0.95$ (the third row), and $\beta = 0.995$ (the last row); $ct/a = 6$ (left column), $ct/a = 12$ (middle column), and $ct/a = 32$ (right column); $\omega_p a/c = 2$, $a/r = 0.5$.

where

$$\beta_1 = (\sqrt{5} - 1)/2 \approx 0.62,$$
$$\beta_2 = \left[2\left(\omega_n^2 + \omega_p^2\right)\left(2\omega_n^2 + \omega_p\left(\omega_p - \sqrt{4\omega_n^2 + \omega_p^2}\right)\right)\right]^{1/2} / 2\omega_n^2. \quad (28)$$

It is interesting that the low velocity limit for this phenomenon does not depend on any of the parameters of the problem.

VII. NUMERICAL RESULTS AND DISCUSSION

Figures 6 and 7 present the behavior of the free electromagnetic field in the vacuum and cold plasma for different velocities of the charge motion, β, and at different moments. Upon analysis of TR, some interesting effects can be visualized. Figure 6 shows the dependence of the radial components E_r of the first (continuous line) and second (dashed line) modes of the free field on distance z/a for different dimensionless time values of ct/a and different velocities β. Note that the vertical scale is different in different figures.

One can see that the behavior of the field near the boundary is rather dramatic and that the second mode can be significant in some areas. It should be underlined that the magnitudes of the field components at $z = 0$ are large but finite. For relatively slow charge velocities, the field in the vacuum is greater than the field in the plasma [Figs. 6(a), 6(b), and 6(c)]. This correlation changes with increases in β. For $\beta = 0.85$ [Figs. 6(d), 6(e), and 6(f)], the fields in the vacuum and plasma are approximately of equal magnitude. For greater velocities, the field in the plasma becomes greater than the field in the vacuum [Figs. 6(g), 6(h), and 6(i)]. Finally, there

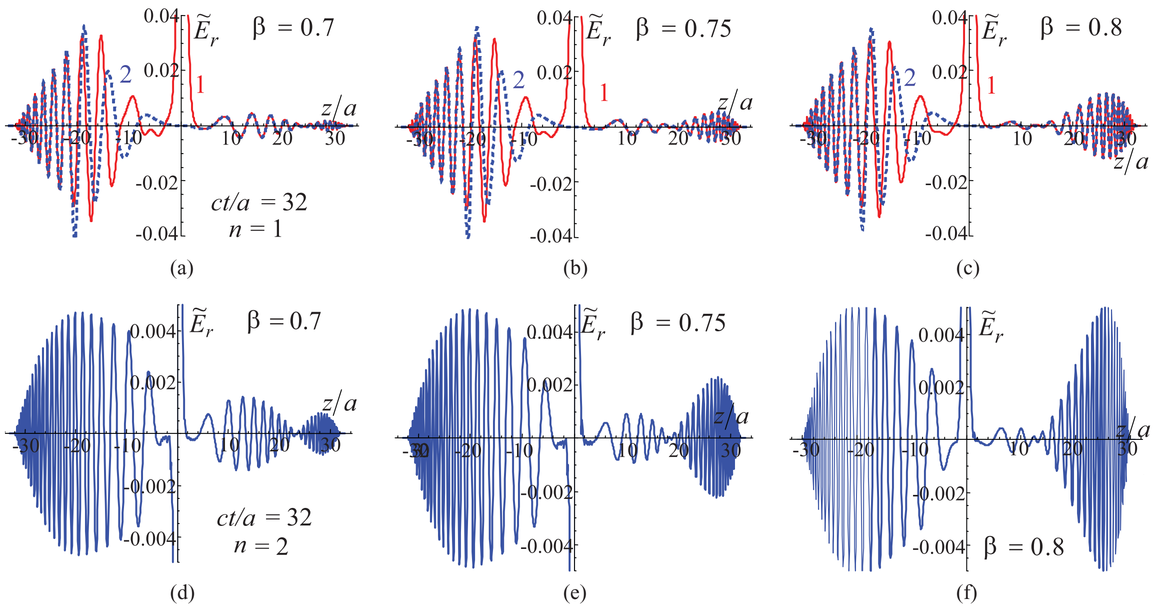

FIG. 7. (Color online) Dependence of normalized transversal component $\widetilde{E}_r$ of the first (top) and second (bottom) modes on distance for $ct/a = 32$ and different values of β. In all of the figures, the result of the exact calculation is shown (solid line 1). For the first mode (top), asymptotic approximations (the saddle point contributions) are given as well (dashed line 2). $\omega_p a/c = 2$, $a/r = 0.5$.

is a considerable increase and concentration of the field near the wave front in the plasma for the case of the ultrarelativistic particle [Figs. 6(j), 6(k), and 6(l)]. So, it could indicate that starting from some velocities of the charge motion, all radiation in the plasma is getting directed forward. Note that this effect can be used for generating electromagnetic radiation.

In addition, there is another interesting physical phenomenon. One can see that the envelope of the field has the zero point at some velocities for the charge's motion, β (Fig. 7). This effect appears near the wave front at the critical value of β_1, moves in the direction of the boundary $z = 0$ with increasing β from β_1 to β_2, and disappears at β_2. β_1 and β_2 are the same for the analogous phenomenon for the energy spectrum of the nth mode of TR. As soon as the zero point of the field envelope appears near the wave front where the frequencies characterized the field are much greater than plasma frequency, the role of medium and waveguide is negligibly small. It might explain the independence of β_1 on any of parameters of the problem. As it follows from (28), the velocity range of this effect is $0.62 < \beta < 0.87$ for the first mode [Figs. 7(a)–7(c)]; for the second mode, it is $0.62 < \beta < 0.89$ [Figs. 7(d)–7(f)].

In Figs. 7(a)–7(c), the results are obtained using two methods (analytical and numerical) at the moment when $ct/a = 32$. The dashed line 2 corresponds to the saddle point contributions. One can see that both methods provide good agreement in a sufficiently wide area. There is a discrepancy

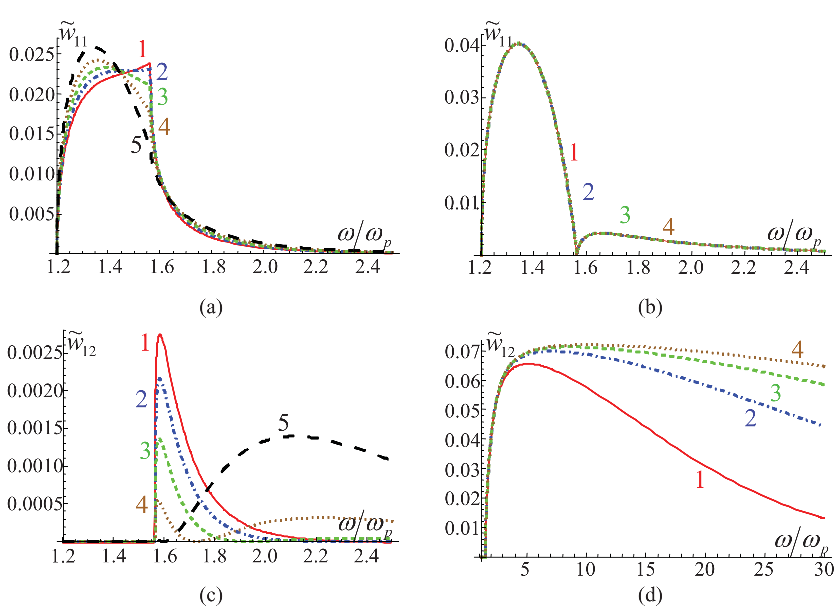

FIG. 8. (Color online) Dependence of the normalized spectral density of energy for the first mode of TR $\widetilde{w}_{11,2} = w_{11,2}\pi c/4q^2$ in the vacuum (top) and plasma (bottom) at a normalized frequency ω/ω_p for different velocities of the charge's motion: (a) and (c) thick solid line 1: $\beta = 0.65$, dot-dashed line 2: $\beta = 0.7$, short dashed line 3: $\beta = 0.75$, dotted line 4: $\beta = 0.8$, and long dashed line 5: $\beta = 0.85$; (b) and (d) thick solid line 1: $\gamma = 30$, dot-dashed line 2: $\gamma = 60$, dashed line 3: $\gamma = 90$, and dotted line 4: $\gamma = 120$; $\omega_p a/c = 2$, $a/r = 0.5$, $\gamma = 1/\sqrt{1-\beta^2}$.

between the analytical and numerical results near the boundary because the asymptotic expressions are not valid if the saddle points are too close to the poles or to the branch points (line 1 presents the exact solution).

Figure 8 shows the behavior of the spectral density of the first mode of transition radiation in the vacuum and cold plasma for different velocities β. As shown before, the energy spectrum of the nth mode of TR in the vacuum is limited from below by ω_n; in the plasma, it exists at higher frequencies of $\omega > \sqrt{\omega_n^2 + \omega_p^2}$. Note that the spectral density of the energy in the vacuum has a break point at $\omega = \sqrt{\omega_n^2 + \omega_p^2}$. In addition, the energy spectral density in the plasma has the zero point when the charge's velocity is within the limits of $\beta_1 < \beta < \beta_2$ [Fig. 8(c)]. This effect correlates with the phenomenon of the zero point of the envelope discussed above.

One can see [Figs. 8(a) and 8(c)] that there is more radiation in the vacuum than in the plasma for relatively low velocities β. However, with increases in β, the energy spectrum in the plasma becomes greater than that in the vacuum. Figures 8(b) and 8(d) represent the dependence of the spectral density in the vacuum and plasma for ultrarelativistic particles. The spectral density in the vacuum does not depend on γ for $\gamma > 30$ [all curves in Fig. 8(b) do not differ]. The spectral density in the plasma increases to a certain magnitude, and then the spectrum width grows. This effect correlates with the phenomenon of the increase in the field near the wave front for $\gamma \to \infty$.

VIII. CONCLUSION

In this paper, we have presented analytical and numerical results describing the field of a charge traveling from a vacuum into cold plasma in a circular waveguide. Asymptotic expressions for the electromagnetic field of each mode in the vacuum and cold plasma have been obtained using the steepest descent technique. Studies of the singularities of integrands have shown that, in a vacuum, there is the surface standing wave (the pole contributions) and the lateral standing wave (the branch cut contributions). In the plasma, surface standing waves and plasma oscillations exist. All of these types of waves only exist near the boundary. The main contribution in the far zone is the space transition radiation determined by the saddle point.

Using the numerical method, the exact integral representations were obtained. An efficient algorithm of computation based on certain transformations of the integration path in the complex plane was also developed. The behavior of the field components depending on distance and time were explored for different charge velocities. Additionally, the energy passing through the cross section of the waveguide in the vacuum and the plasma was investigated.

Some interesting physical effects are noted. It is shown that, in the plasma, the envelope of the field mode and the energy spectrum density show the zero point when the charge's velocity is within certain limits. Likewise, an important effect has been noted for the case of ultrarelativistic particles, i.e., the field in the plasma increases and concentrates near the wave front if the Lorentz factor γ takes on a large value. This phenomenon can be used for generating electromagnetic fields. Note that such a generator can be realized not only with an ordinary plasma but also with some metamaterials, for example, structures with crossed wires [31]. It is essential that metamaterial is stable in contrast to plasma.

ACKNOWLEDGMENTS

This research was supported by the Education Agency of the Russian Federation.

[1] V. L. Ginzburg and I. M. Frank, Zh. Exps. Teor. Fiz. **16**, 15 (1946).
[2] V. L. Ginzburg and V. N. Tsytovich, *Transition Radiation and Transition Scattering* (Hilger, London, 1990), p 445.
[3] K. A. Barsukov, Zh. Exps. Teor. Fiz. **37**, 1106 (1959).
[4] K. A. Barsukov, Zh. Tekh. Fiz. **30**, 1337 (1960).
[5] S. N. Galyamin, A. V. Tyukhtin, A. D. Kanareykin, and P. Shoessow, Phys. Rev. Lett. **103**, 194802 (2009).
[6] S. N. Galyamin and A. V. Tyukhtin, Phys. Rev. B **81**, 35134 (2010).
[7] S. N. Galyamin, T. Yu. Alekhina, A. V. Tyukhtin, and E. G. Doil'nitsina, in *Proceedings of the International Conference "Days on Diffraction," 2009, St. Petersburg, Russia*, edited by I. V. Andronov *et al.* (St. Petersburg University, St. Petersburg, 2009), pp. 69–75.
[8] S. N. Galyamin and A. V. Tyukhtin, J. Phys.: Conf. Ser. **236**, 012003 (2010).
[9] I. M. Frank, *Vavilov-Cherenkov Radiation: Theoretical Aspects* (Nauka, Moscow, 1988), p 288 (in Russian).
[10] G. N. Afanasiev and V. G. Kartavenko, J. Phys. D **31**, 2760 (1998).
[11] G. N. Afanasiev, V. G. Kartavenko, and E. N. Maga, Physica B **269**, 95 (1999).
[12] A. V. Tyukhtin and S. N. Galyamin, Phys. Rev. E **77**, 066606 (2008).
[13] B. M. Bolotovskiy, Usp. Fiz. Nauk. **75**, 295 (1961).
[14] W. Gai, P. Schoessow, B. Cole, R. Konecny, J. Norem, J. Rosenzweig, and J. Simpson, Phys. Rev. Lett. **61** 24, 2756 (1988).
[15] J. G. Power, W. Gai, and P. Schoessow, Phys. Rev. E **60**, 6061 (1999).
[16] A. M. Altmark, A. D. Kanareykin, and I. L. Sheinman, J. Tech. Phys. **50**, 87 (2005).
[17] C. Jing, A. D. Kanareykin, J. G. Power, M. Conde, Z. Yusof, P. Schoessow, and W. Gai, Phys. Rev. Lett. **98**, 144801 (2007).
[18] A. V. Tyukhtin, Tech. Phys. Lett. **30**, 605 (2004).
[19] A. V. Tyukhtin, Tech. Phys. Lett. **31**, 150 (2005).
[20] A. D. Kanareykin and A. V. Tyukhtin, Nucl. Instrum. Methods Phys. Res., Sect. A **558**, 62 (2006).
[21] L. Schächter, Phys. Rev. E **62**, 1252 (2000).
[22] S. Banna, V. Berezovsky, and L. Schächter, Phys. Rev. E **74**, 046501 (2006).

[23] N. V. Ivanov and A. V. Tyukhtin, Tech. Phys. Lett. **32**, 449 (2006).
[24] A. V. Tyukhtin, A. D. Kanareykin, and P. Schoessow, Phys. Rev. ST Accel. Beams **10**, 051302 (2007).
[25] S. Antipov, L. Spentzouris, W. Liu, W. Gai, and J. G. Power, J. Appl. Phys. **102**, 034906 (2007).
[26] A. V. Tyukhtin, Tech. Phys. Lett. **34**, 884 (2008).
[27] A. V. Tyukhtin, Tech. Phys. Lett. **35**, 263 (2009).
[28] L. M. Brekhovskih, *Waves in Layered Media* (Academic, New York, 1980).
[29] B. Felsen and N. Marcuvitz, *Radiation and Scattering of Waves* (Wiley Interscience, Hoboken, 2003), p. 888.
[30] V. N. Krasilnikov and A. V. Tyukhtin, Radiophysics and Quantum Electronics **30**, 818 (1987).
[31] J. B. Pendry, A. J. Holden, W. J. Stewart, and I. Youngs, Phys. Rev. Lett. **76**, 4773 (1996).